Evidence for the Interaction of A$_3$ Adenosine Receptor Agonists at the Drug-Binding Site(s) of Human P-glycoprotein (ABCB1)[S]

Biebele Abel, Dilip K. Tosh, Stewart R. Durell, Megumi Murakami, Shahrooz Vahedi, Kenneth A. Jacobson, and Suresh V. Ambudkar

Laboratory of Cell Biology, Center for Cancer Research, National Cancer Institute (B.A., S.R.D., M.M., S.V., S.V.A.), and Molecular Recognition Section, Laboratory of Bioorganic Chemistry, National Institute of Diabetes and Digestive and Kidney Diseases (D.K.T., K.A.J.), National Institutes of Health, Bethesda, Maryland

ABSTRACT

P-glycoprotein (P-gp) is a multidrug transporter that is expressed on the luminal surface of epithelial cells in the kidney, intestine, bile-canalicular membrane in the liver, blood-brain barrier, and adrenal gland. This transporter uses energy of ATP hydrolysis to efflux from cells a variety of structurally dissimilar hydrophobic and amphipathic compounds, including anticancer drugs. In this regard, understanding the interaction with P-gp of drug entities in development is important and highly recommended in current US Food and Drug Administration guidelines. Here we tested the P-gp interaction of some A$_3$ adenosine receptor agonists that are being developed for the treatment of chronic diseases, including rheumatoid arthritis, psoriasis, chronic pain, and hepatocellular carcinoma. Biochemical assays of the ATPase activity of P-gp and by photolabeling P-gp with its transport substrate [^{125}I]-iodoarylazidoprazosin led to the identification of rigidified (N)-methanocarba nucleosides (i.e., compound **3** as a stimulator and compound **8** as a partial inhibitor of P-gp ATPase activity). Compound **8** significantly inhibited boron-dipyrromethene (BODIPY)-verapamil transport mediated by human P-gp (IC$_{50}$ 2.4 ± 0.6 μM); however, the BODIPY-conjugated derivative of **8** (compound **24**) was not transported by P-gp. In silico docking of compounds **3** and **8** was performed using the recently solved atomic structure of paclitaxel (Taxol)-bound human P-gp. Molecular modeling studies revealed that both compounds **3** and **8** bind in the same region of the drug-binding pocket as Taxol. Thus, this study indicates that nucleoside derivatives can exhibit varied modulatory effects on P-gp activity, depending on structural functionalization.

SIGNIFICANCE STATEMENT

Certain A$_3$ adenosine receptor agonists are being developed for the treatment of chronic diseases. The goal of this study was to test the interaction of these agonists with the human multidrug resistance-linked transporter P-glycoprotein (P-gp). ATPase and photolabeling assays demonstrated that compounds with rigidified (N)-methanocarba nucleosides inhibit the activity of P-gp; however, a fluorescent derivative of one of the compounds was not transported by P-gp. Furthermore, molecular docking studies revealed that the binding site for these compounds overlaps with the site for paclitaxel in the drug-binding pocket. These results suggest that nucleoside derivatives, depending on structural functionalization, can modulate the function of P-gp.

Introduction

P-glycoprotein (P-gp; ABCB1) is a member of the ATP-binding cassette (ABC) superfamily, which has a role in drug resistance. P-gp is expressed on the luminal surface of the epithelial cells in the intestine, kidney, bile-canalicular membranes in the liver, blood-brain barrier, and adrenal gland. P-gp is believed to protect these tissues from xenobiotic accumu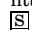lation, which can result in toxicity (Leslie et al., 2005). This multidrug transporter is a single-polypeptide chain with a molecular weight of ~170 kDa, and it comprises two transmembrane domains (TMDs) and two nucleotide-binding domains located in the plasma membrane (Gottesman and Pastan, 1993; Ambudkar et al., 1999). These domains of P-gp function as a unit to transport substrates across the plasma membrane. The TMD comprises six transmembrane helices, and the nucleotide binding domain comprises the A-loop, the Walker A and Walker B motifs, the signature motif (also identified as the C motif with consensus sequence LSGGQ), and the D- and H-loops. Additionally, P-gp is known to interact with various types and sizes of hydrophobic compounds, including natural products, chemotherapeutic drugs, steroids, linear and cyclic peptides, and fluorescent dyes. Because of the hydrophobic nature of these compounds, they can easily cross the plasma membrane and penetrate tissues and other pharmacologic compartments. In this regard, understanding the interaction of these compounds

ABBREVIATIONS: ABC, ATP-binding cassette; BD, BODIPY; BODIPY, boron-dipyrromethene; DMF, dimethylformamide; FBS, fetal bovine serum; IAAP, [^{125}I]-iodoarylazidoprazosin; IMDM, Iscove's modified Dulbecco's medium; P-gp, P-glycoprotein; TMD, transmembrane domain.

with P-gp is important for drug design. Furthermore, Food and Drug Administration guidelines for drug design recommend that new drugs be tested in vitro to determine whether they are potential substrates of P-gp.

A₃ adenosine receptor agonists are being developed for treatment of chronic diseases, including rheumatoid arthritis, psoriasis, chronic pain, and hepatocellular carcinoma (Tosh et al., 2012b, 2014b, 2015b). These nucleoside derivatives are typically based on an adenosine scaffold that is modified at multiple positions. One such agonist that is highly potent and selective at the A₃ receptor, compound **3**, showed efflux (ratio 86) in a Caco-2 cell bidirectional transport model (Tosh et al., 2015b), suggesting a possible interaction with P-gp or a related pump in the intestinal epithelium. Therefore, we examined the effects on P-gp ATPase activity of a series of structurally varied adenosine derivatives (Tosh et al., 2012a,b, 2014b, 2015a,c, 2016, 2017), many of which are potent A₃ adenosine receptor agonists and selective for that receptor subtype. Many of these analogs contain, in place of ribose, a rigid (N)-methanocarba ([3.1.0]bicyclohexyl) ring system, which has been shown to enhance potency and selectivity at the A₃ adenosine receptor. We also synthesized new nucleoside derivatives designed for P-gp interactions, as indicated by the structure activity relationship analysis and modeled binding mode in the drug-binding pocket of P-gp.

In this study, we investigated the interaction of P-gp with some of the adenosine receptor agonists that have been developed for the treatment of chronic diseases. We discovered that most adenosine receptor ligands neither stimulated nor inhibited the basal ATPase activity, suggesting the loss of their affinity toward P-gp. Although compounds **3** and **8** displayed pronounced effects on P-gp function, we found that a BODIPY-conjugate of compound **8** (compound **24**) was not transported by P-gp. Using a recently solved atomic structure of paclitaxel (Taxol, Pfizer, New York, NY)-bound human P-gp (Alam et al., 2019) (pdb. 6QEX), in silico docking simulations were performed to identify candidate contacting residues in the drug-binding pocket. We compared the results for Taxol and compounds **3** and **8**. We found that 18 of 26 residues showed interaction with both compound **3** and Taxol, whereas 23 of 26 residues are common with compound **8** and Taxol. The docking studies indicate that the binding site for both compounds **3** and **8** overlaps with the site for Taxol. Collectively, these results suggest that A₃ adenosine receptor agonists modulate the function of P-gp.

Materials and Methods

Chemicals. Dimethylsulfoxide, sodium butyrate compounds **22** and **23**, and other chemicals, unless specified, were obtained from Sigma Chemical Co. (St. Louis, MO). [¹²⁵I]-Iodoarylazidoprazosin (1100 Ci/mmol) was obtained from PerkinElmer Life Sciences (Wellesley, MA). Fluorescent substrates used in this work, tetramethylrosamine chloride, BODIPY (BD)-verapamil, daunorubicin, BODIPY FL hydrazide (4,4-difluoro-5,7-dimethyl-4-bora-3a,4a-diaza-*s*-indacene-3-propionic acid, hydrazide), and rhodamine 123 were all purchased from Invitrogen/ThermoFisher (Carlsbad, CA).

Chemical Synthesis. The synthetic routes to compounds **7**, **8**, and **24** are shown in Figs. 1 and 2. The experimental details can be found in the Supplemental Methods. Other nucleoside derivatives were synthesized as reported: **1–4**, **20** (Tosh et al., 2012a); **5**, **6**, and **12** (Tosh et al., 2016); **9–11** (Tosh et al., 2014b); **13** (Tosh et al., 2015b); **14** (Tosh et al., 2015a); **15–17** (Tosh et al., 2017); **19** (Tosh et al., 2012b); **18** and **21** (Tosh et al., 2015c).

Preparation of Total Membranes from High-Five Insect Cells. Total membrane vesicles were prepared by hypotonic lysis of High-Five (ThermoFisher) insect cells expressing P-gp and differential centrifugation, as previously described (Sauna and Ambudkar, 2000; Kerr et al., 2001). Cells (Invitrogen) were infected with recombinant baculovirus carrying human wild-type or mutant P-gps with a 6XHis-tag site at the C-terminal end, as previously described (Ramachandra et al., 1998).

ATPase Activity of P-gp. Human P-gp–mediated ATPase activity was measured using methods we described previously (Ambudkar, 1998). P-gp–specific activity was measured as vanadate-sensitive ATPase activity. In this procedure, wild-type or mutant P-gp (10 μg) was preincubated with the indicated compounds in the presence and absence of sodium orthovanadate using ATPase 2× buffer containing 50 mM MES-Tris (pH 6.8), 50 mM KCl, 10 mM MgCl₂, 5 mM NaN₃, 1 mM EGTA, 1 mM ouabain, and 2 mM DTT. The reaction was then started by the addition of 5 mM ATP and stopped by the addition of SDS (final concentration, 2.5%), and the inorganic phosphate generated over 20 minutes at 37°C was measured using colorimetric reaction (Ambudkar, 1998). Three independent experiments in duplicate were carried out, and the results are reported as mean ± S.D.

Photolabeling of Human P-gp with ¹²⁵IAAP. The photoaffinity labeling of P-gp with [¹²⁵I]-iodoarylazidoprazosin (¹²⁵IAAP) was carried out using total membranes of High-Five insect cells expressing human P-gp (60 μg of protein per 100 μl). The protein was then incubated at room temperature for 5 minutes with the indicated concentrations of compounds **3** or **8**. The samples were later transferred to a 4°C water bath before the addition of ¹²⁵IAAP (3 to 4 nM), followed by photo-crosslinking with 366-nm UV light for 10 minutes under subdued light at room temperature. Subsequently, protein bands were separated using gel electrophoresis, and quantification of IAAP incorporation into P-gp bands was achieved as described previously (Sauna et al., 2006).

Cell Line and Culture Conditions. HeLa cells were obtained from American Type Culture Collection (Manassas, VA). The cells were later maintained in Dulbecco's modified Eagle's medium supplemented with 10% fetal bovine serum (FBS) solution, 5 mM L-glutamine, 50 U/ml penicillin, and 50 μg/ml streptomycin at 37°C (Kapoor et al., 2013).

Transduction of Hela Cells with BacMam-P-gp Baculovirus. HeLa cells were transduced with the human P-gp BacMam baculovirus at a titer of 30–100 virus particles per cell, as we described previously (Shukla et al., 2012). HeLa cells (3 × 10⁵/tube) were analyzed for cell surface expression of P-gp by incubation with the human P-gp–specific monoclonal antibody MRK16 (1 μg per 100,000 cells) for 30 minutes in Iscove's modified Dulbecco's medium (IMDM; Difco) containing 5% FBS at 37°C. The cells were later washed with cold IMDM and incubated with fluorescein isothiocyanate–labeled antimouse secondary antibody IgG2aκ (0.25 μg/100,000 cells) at 37°C. We later washed the cells with cold IMDM after incubation and resuspended them in cold PBS containing 1% bovine serum albumin. The stained cells were analyzed by flow cytometry using a FACS CANTO II instrument with BD FACSDiva software (BD Biosciences, Franklin Lakes, NJ), and the data were analyzed using FlowJo software (Tree Star, Inc., Ashland, OR).

Transport Assay. The effect of compound **8** on the transport function of human P-gp was determined using flow cytometry. In this assay, human P-gp, 3 × 10⁵ HeLa cells in IMDM medium containing 5% FBS, were incubated with fluorescent substrate (BD-verapamil at final concentration at 0.5 μM). The cells were then incubated with BD-verapamil for 45 minutes at 37°C. After incubation, the cells were washed with cold IMDM and resuspended in cold PBS containing 1% BSA. The transport of BD-verapamil was measured by flow cytometry using untransduced cells as our control in this experiment. The mean fluorescence intensity of P-gp–expressing cells after subtraction from that of untransduced cells was taken as 100% efflux. Each substrate was tested three times, and the results were analyzed as described previously (Shukla et al., 2012).

Docking of Compounds 3 or 8 in the Drug-Binding Pocket of Human P-gp. Docking simulations were conducted with the
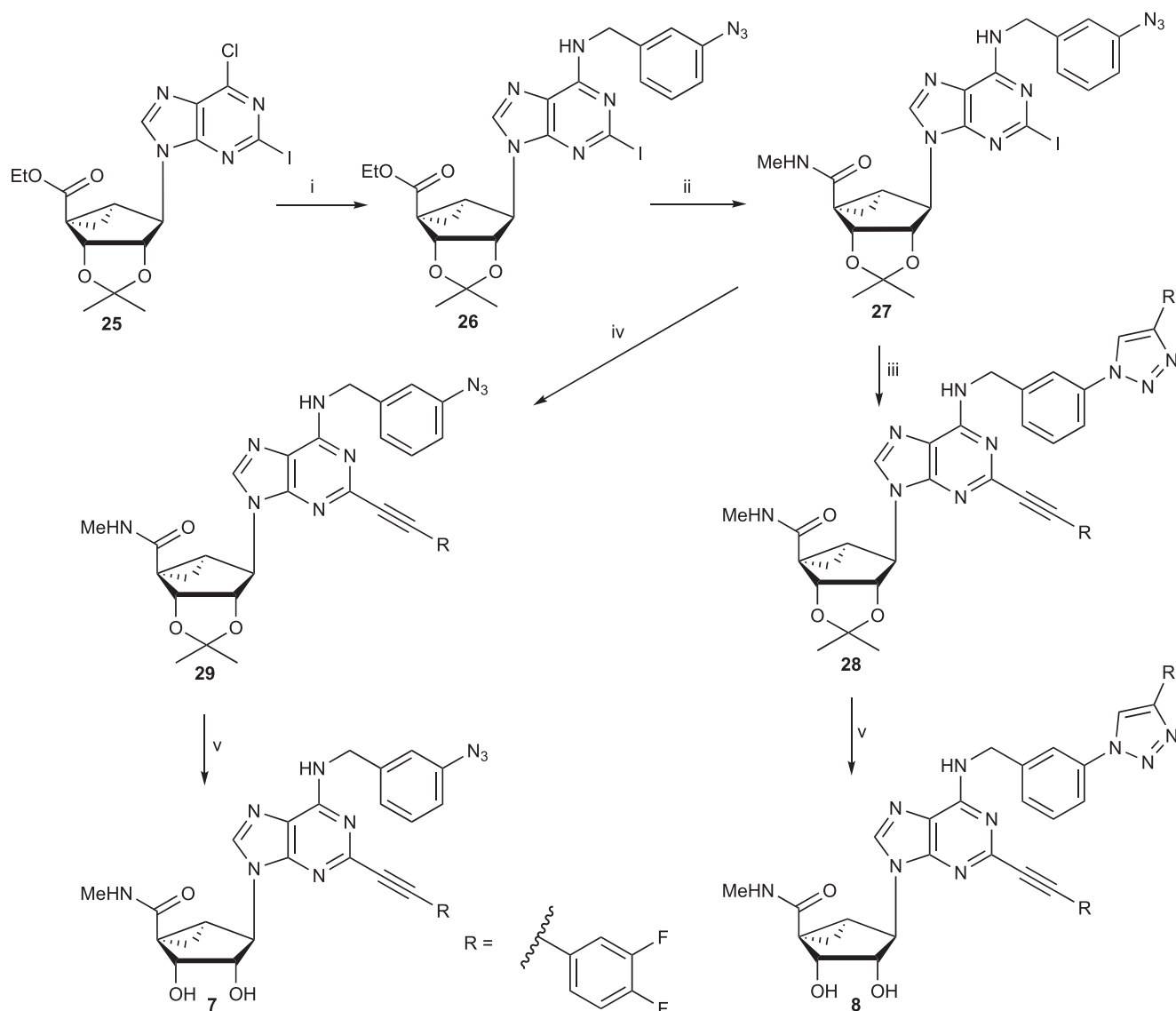
Fig. 1. Synthesis of compounds **7** and **8**. Reagents and conditions: (i) 3-azido-benzylamine Et₃N, MeOH; (ii) 40% methylamine, MeOH, rt.; (iii) arylethyne, Pd(PPh₃)₂Cl₂, CuI, Et₃N, DMF, rt.; (iv) arylethyne, Pd(PPh₃)₂Cl₂, Et₃N, DMF, rt.; (v) 10% trifluoroacetic acid, H₂O, 70°C.

AutoDock Vina software (Trott and Olson, 2010). The model of the protein receptor was derived from the recent cryoelectron microscopy–determined structure of human P-gp with bound transport substrate Taxol (Alam et al., 2019) (pdb.6QEX). In the simulations, the following 42 lumen-facing amino acid sidechains in the outer, narrower portion of the transmembrane domain were allowed to rotate: L65, F72, M192, Q195, S196, T199, S222, N296, I299, F303, I306, Y307, Y310, F335, F336, L339, I340, F343, S344, V345, Q347, N721, Q725, F728, F732, I736, Q773, I868, Q946, M949, Y950, Y953, F957, L975, F978, S979, V982, F983, M986, Q990, S993 and F994. All rotatable, single bonds of the ligands were also allowed to vary. The 1.0 Å-spacing search grid was centered over this region with dimensions 36 × 40 × 40 Å. The simulations were run with an exhaustiveness parameter of 200 on the National Institutes of Health high-performance computing system (NIH HPC Biowulf cluster; (http://hpc.nih.gov).

Results

Chemistry. The synthesis of novel nucleosides studied here (i.e., **7**, **8**, and **24**) is shown in Figs. 1 and 2, and the

procedures and data confirming the assigned structures are provided in the Supplemental Methods. Nucleoside derivative **25** was treated with 3-azido-benzylamine in the presence of triethylamine, resulting in the N^6-benzyl derivative **26**. Sonogashira reaction of compound **26** with 3,4-difluoro-phenylethyne delivered an unusual product **28**, which had an aryl group that entered a "click" reaction with the azido group of the N^6-benzyl moiety. This reaction occurred because of the presence of CuI in the Sonogashira condition. Deprotection of the isopropylidene group of compound **28** in 10% trifluoroacetic acid afforded compound **8**. To get the Sonogashira coupling product, the reaction was further attempted with compound **27** in the absence of CuI, and the desired compound **29** was obtained exclusively. Acid hydrolysis of compound **29** produced compound **7**. Fluorescent boron-dipyrromethene (BODIPY) derivative **30** was coupled with 3-ethynyl-benzoic acid in the presence of 1-[bis(dimethylamino)methylene]-1H-1,2,3-triazolo[4,5-b]pyridinium 3-oxide hexafluorophosphate (HATU) and N,N-diisopropylethylamine (DIPEA), resulting in the BODIPY-alkyne derivative **31**, which clicked with the azido
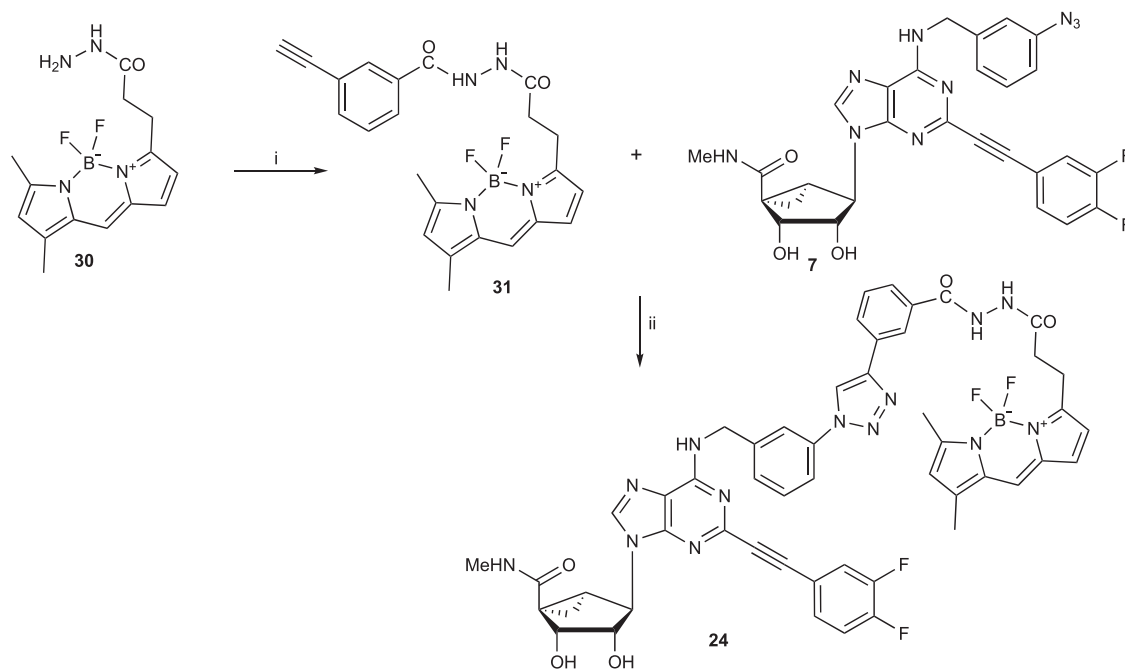
Fig. 2. Synthesis of compound **24** by click chemistry coupling. Reagents and conditions: (i) 3-ethynyl-benzoic acid, HATU, DIPEA, DMF, rt.; (ii) sodium ascorbate, $CuSO_4 \cdot 5H_2O$, DMF, H_2O, rt.

compound **7** in the presence of sodium ascorbate and copper sulfate to afford the BODIPY-conjugated nucleoside derivative **24** (Fig. 2).

Structural-ATPase Activity Relationship. To investigate the interaction of A₃ adenosine receptor agonists at the drug-binding pocket of P-gp, the effect of selected nucleosides on ATPase activity of the transporter was determined. In this work, a set of 23 novel and known adenosine receptor ligands was synthesized and tested at various concentrations (e.g., 2.5 and 10 μM) using total membranes from High-Five insect cells expressing human P-gp. The adenosine analogs were tested for their ability to either stimulate or inhibit the basal ATPase activity of P-gp. Furthermore, we interpreted the ATPase activity of P-gp as follows: 1) adenosine analogs stimulating basal ATPase activity are mostly transporter substrates; 2) analogs that show no effect on basal ATPase activity suggest no interaction with P-gp; and 3) nucleosides that inhibit the basal ATPase activity of P-gp are most likely able to inhibit its transport function. In this section, all results were reported as a percentage of the ATPase activity of P-gp, with values below or equal to 30% considered ineffective, unless otherwise specified.

To analyze the structure-activity relationship, we grouped the A₃ adenosine receptor agonists into three structural categories: 1) (N)-methanocarba 2-phenylethynyl-purine derivatives, including 2-(3,4-difluorophenylethynyl)-N^6-3-chlorobenzyl adenosine derivative compound **3**; 2) purine (N)-methanocarba and riboside analogs containing a 2-(5-chlorothienyl-ethynyl) group, which are potent A₃AR agonists; and 3) various intact and truncated adenosine (N)-methanocarba and riboside derivatives, including two A₃AR agonists, **22** and **23**, which are currently in phase 2 and 3 clinical trials. In this ATPase assay, we used zosuquidar, which is a high-affinity modulator of P-gp in native membranes, as our positive control.

Initially, we tested an N^6-3-chlorobenzyl-2-(3,4-difluorophenylethynyl)-(N)-methanocarba adenosine derivative with R^1

substitution being N^6-(3-chlorobenzyl) and R^2 a phenyl group (compound **1**). This compound was observed to show weak stimulation of basal ATPase activity of P-gp at 2.5 and 10.0 μM. To attempt to increase the hydrogen bonding, π-π, or van der Waals interactions between the ligands and residues in the transmembrane region of P-gp, we then tested analogs with a halogen atom on the phenyl ring, and the results obtained are shown in Table 1. We observed from the results that compound **2,** which consists of R^1:N^6-(3-chlorobenzyl) and R^2: 4-fluorophenyl, showed no effect on the basal ATPase activity of P-gp; however, compound **3,** which contains R^1: N^6-(3-chlorobenzyl) and R^2: 3,4-difluorophenyl, showed stimulation of ATPase activity up to 2-fold, at concentrations ranging from 2.5 to 5.0 μM, with EC_{50} value of 0.45 $\pm$ 0.22 μM (Fig. 3A). At higher concentrations, compound **3** showed loss of affinity toward P-gp at concentrations ranging from 6.0 to 10.0 μM (data not shown). This change in affinity is possibly due to the flexible nature of the drug-binding pocket of P-gp and because there are multiple binding sites in this region for a given substrate (Chufan et al., 2013). Most modulators of P-gp bind to the primary or high-affinity drug-binding site of the protein at low concentrations; however, at high concentrations, they can bind to an alternative or secondary low-affinity site. This result could explain the reason for the switch from stimulation at low concentration to no effect of basal ATPase activity at higher concentrations for compound **3**. Additionally, compound **4** (R^1: N^6-(3-chlorobenzyl), R^2: 5-chlorophenyl), **5** (R^1: hydrogen, R^2: 3, 4-difluorophenyl), **6** (R^1: methyl, R^2: 3, 4-difluorophenyl), and **7** (R^1:azido phenyl, R^2: 3, 4-difluorophenyl) all showed loss of affinity toward P-gp, suggesting that substituting these groups at position R^1 allows for weak interaction with the protein. We then decided to synthesize a compound with structural features identical to known high-affinity inhibitors of P-gp such as tariquidar, zosuquidar, and elacridar. In this regard, compound **8** was

TABLE 1
Effect of (N)-methanocarba 2-phenylethynyl-purine derivatives on ATPase activity of P-gp

A summary of the effect of (N)-methanocarba 2-phenylethynyl-purine derivatives, including 2-(3,4-difluorophenylethynyl)-N^6-3-chlorobenzyl adenosine derivative compound **3**, on the ATPase activity of P-gp. Modulation of the basal ATPase activity of P-gp by adenosine derivation was done at 2.5 and 10 μM. The percentage of stimulation or inhibition by indicated compounds is shown. ATPase activities were determined as described in *Materials and Methods*. The values in the ATPase activity column indicate stimulation (upward arrow) or inhibition (downward arrow) of basal ATPase activity. Values represent mean ± S.D. of three independent experiments. ATPase activity was measured in total membranes prepared from High-Five insect cells expressing human or mutant P-gp. Membranes (10 μg of protein/100 μl) were incubated with indicated concentrations of compounds, in the presence and absence of sodium orthovanadate (0.3 mM), in ATPase assay buffer as previously described (Ambudkar, 1998). Basal ATPase activity is considered as "0" %. Zosuquidar was used as a positive control, which showed inhibition of ATPase activity as 85% at 2.5 μM. The effects on the basal ATPase activity below or equal to 30% are indicated as NE, no effect, and ND, not determined.
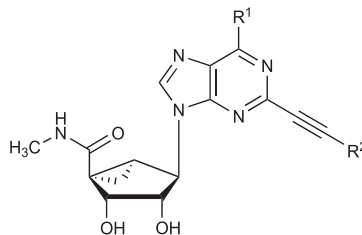
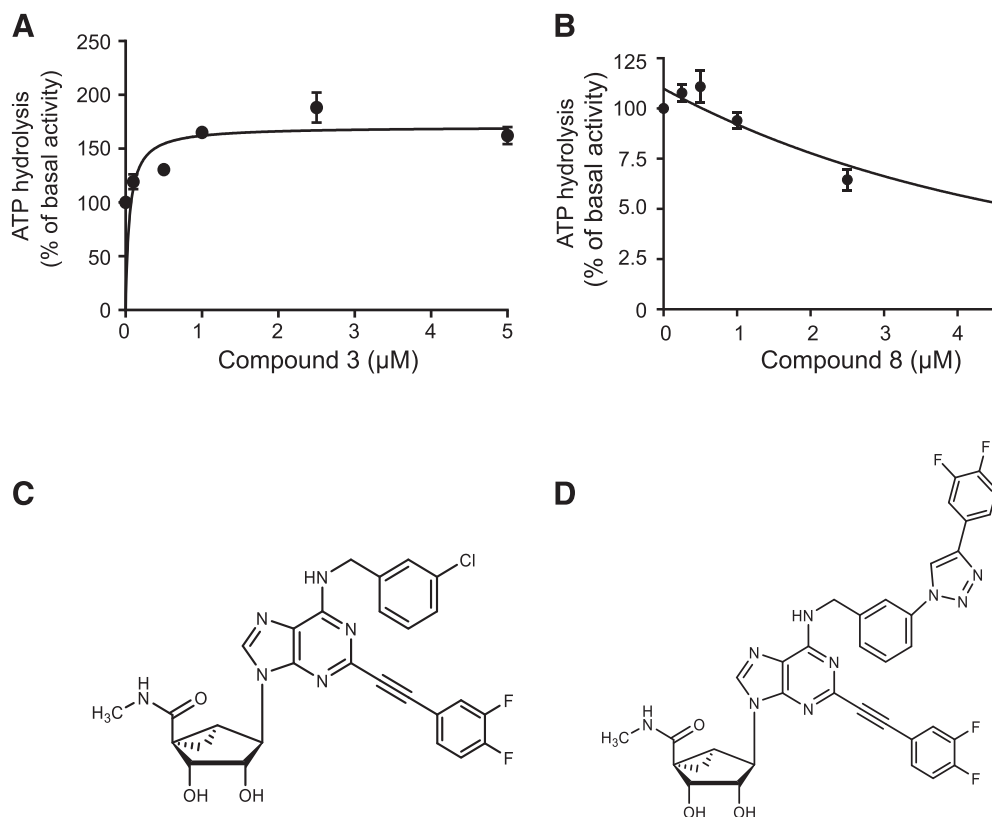| No.	R^1	R^2	ATPase Activity of P-gp % Stimulation or Inhibition	
			2.5 μM	10 μM
1			30.4 ± 7.2 ↑	31.0 ± 5.3 ↑
2			NE	NE
3			88.3 ± 14.0 ↑	NE
4			NE	NE
5	H		NE	NE
6	CH$_3$		NE	NE
7			NE	ND
8			35.4 ± 4.4 ↓	48.2 ± 12.3 ↓
9			NE	41.5 ± 7.1 ↓
10			NE	52.6 ± 8.5 ↓
11			NE	51.3 ± 3.0 ↓

Fig. 3. Effect of compounds 3 (A) and 8 (B) on the ATPase activity of P-gp. The total membranes of High-Five insect cells expressing human P-gp were used for the ATPase assay as described in the *Materials and Methods* section. The curves represent the mean ± S.D. values from three independent experiments performed in duplicate. The EC_{50} = 0.45 ± 0.22 μM, shown in (A), and the IC_{50} = 3.18 ± 0.017 μM, shown in (B), were calculated using GraphPad Prism 7.0 (GraphPad Software, San Diego, CA). The chemical structures of compound **3** (C) and **8** (D) are shown.

synthesized with an extended 3-substituted benzyl at positions R^1 and R^2, which consisted of a 3,4-difluorophenyl, which increased the hydrogen bonding or π-π interactions with residues in the drug-binding pocket of P-gp; however, our results indicated that compound **8** showed partial inhibition of basal ATPase activity of P-gp with an IC_{50} value of 3.18 ± 0.17 μM. The extent of inhibition increased as the concentration of compound increased (Fig. 3B). To increase the inhibitory effect of adenosine analogs (compound **8**), we synthesized 2-(3,4-difluorophenylethynyl)-N^6-3-chlorobenzyl (N)-methanocarba adenosine derivatives by replacing the position R^2, initially 3, 4-difluorophenyl for compound **8** with a phenyl group in the case of compounds **9**, **10**, and **11**. These compounds showed weak inhibition of basal ATPase activity of P-gp at 10 μM, suggesting fluorine atoms at position R^2 are essential for increased affinity toward P-gp (Table 1). As shown in Table 1, the chemical structures of compounds **10** and **11** are diastereomers of compound **9**, and they differ only by their stereochemistry. The graph plots for compounds **9** (A), **10** (B), and **11** (C) (Supplemental Fig. 1) show that basal ATPase activity of P-gp was inhibited in a concentration-dependent manner, with IC_{50} values for compounds **9** (3.69 ± 0.03 μM, **10** (5.27 ± 0.02 μM), and **11** (4.45 ± 0.03 μM), respectively. Furthermore, we selected (N)-methanocarba and ribose analogs of A$_3$AR, which have been previously screened for treating chronic neuropathic pain (Tosh et al., 2014a). These analogs are characterized by their conformationally rigid ribose substitution consisting of a [3.1.0]bicyclohexane (methanocarba) ring system. In this ATPase assay result, we observed that

most of the rigid ribose analogs (**12**, **14**, **16**, and **17**) had no effect on the basal ATPase activity of P-gp. These analogs consist of chemical structures with a methanocarba ring system at position R^2 and a hydrogen atom at position R^1 (compound **12**), and an ethyl methylamine at position R^1 (compound **14**) (Table 2). A similar effect on the ATPase activity was observed for compounds with ribose at position R^2, which also contain methylamine at position R^1 in compound **16** and ethyl methylamine at position R^1 in compound **17**. In addition, an adenosine analog with an R^2: amide methanocarba ring system stimulates the basal ATPase activity of P-gp up to 2-fold in compound **13** (R^1:methylamine) but showed weak stimulation with an R^2: ester methanocarba ring system in compound **15** (R^1:methylamine) (Table 2). The concentration-dependent plot for compound **15** (Supplemental Fig. 2A) shows that as the compound concentration was increased, the stimulation of basal ATPase activity also increased, but maximum stimulation was observed at 5 μM.

Subsequently, we designed additional analogs with the goal of improving their interaction with P-gp by modifying current analogs that either stimulate or partially inhibit the basal ATPase activity. For this reason, compounds **18**, **19**, and **20** were synthesized with structural features similar to those of compound **3** that stimulate ATPase activity. Compound **18**, with an azido group at position R^2, showed no effect on the basal ATPase activity of P-gp at 2.5 μM (Table 3). It is clear, from the concentration-dependent plot for compound **18** (Supplemental Fig. 2B), that as the compound concentration was increased, the stimulation of basal ATPase activity also

TABLE 2
Effect of purine (N)-methanocarba and riboside analogs containing a 2-(5-chlorothienyl-ethynyl) group on the ATPase activity of P-gp

Some of the purine (N)-methanocarba and riboside analogs containing a 2-(5-chlorothienyl-ethynyl) group, which are potent A_3AR agonists, stimulated the ATPase activity of P-gp. ATPase activity was measured in total membranes prepared from High-Five insect cells expressing wild-type or mutant P-gp. ATPase assays were performed as described in *Materials and Methods*. Mean $\pm$ S.D. values represent the average of three independent experiments performed in duplicate. The values in the ATPase activity column indicate stimulation (upward arrow) of basal ATPase activity. Other details are same as given in the caption to Table 1. ND, not determined; NE, no effect.
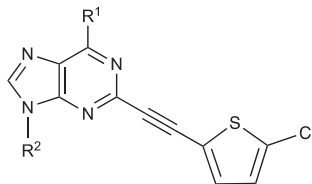
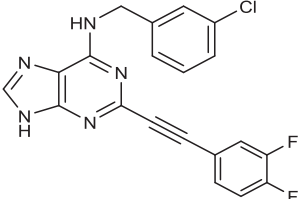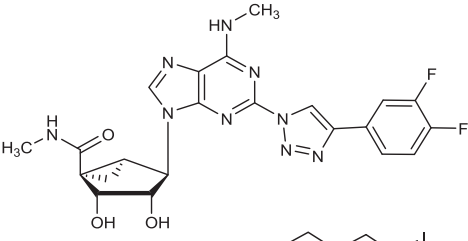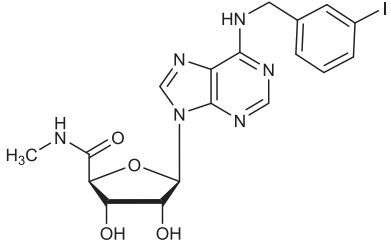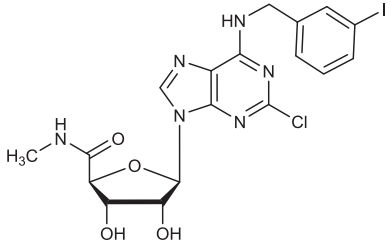| No.	R^1	R^2	ATPase Activity of P-gp % Stimulation or Inhibition	
			2.5 μM	10 μM
12	H		NE	ND
13	$NHCH_3$		115.5 ± 4.9 ↑	NE
14	$NHCH_2CH_2CH_3$		NE	ND
15	$NHCH_3$		37.8 ± 5.0 ↑	ND
16	$NHCH_3$		NE	ND
17	$NHCH_2CH_2CH_3$		NE	ND
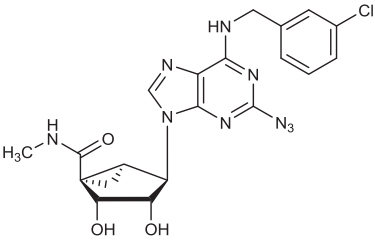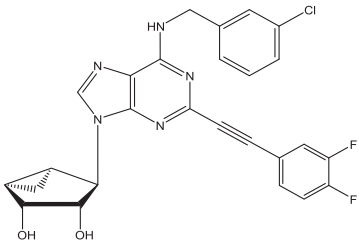
increased, but maximum stimulation was observed at 5 μM, compared with compound **3**, which has an EC_{50} value of 0.45 μM. We then tested compound **19**, which has a 3,4-difluorophenyl moiety at position R^2, and a methanocarba ring system without an amide group at position R^1. This compound showed 2-fold greater stimulation of basal ATPase activity of P-gp at 2.5 μM. These results reveal the importance of a 3,4-difluorophenyl moiety at position R^2 for interaction with P-gp. To observe the importance of the methanocarba ring system with variation at position R^1, we later synthesized an analog without the methanocarba ring system but with a 3,4-difluorophenyl moiety at position R^2 (compound **20**). This

compound, unlike **19**, had no effect on the basal ATPase activity of P-gp, showing the importance of the methanocarba ring system. We also synthesized compound **21** with structural features similar to those of compound **8**, which inhibits the basal ATPase activity of P-gp. Compound **21** has the alkyne group of **8** replaced with triazole at position R^2, and a methyl group takes the place of the extended 3-substituted benzyl of **8** at position R^1. These modifications led to weak stimulation of ATPase activity by compound **21** at 2.5 μM. Thus, to maintain the inhibitory effect of adenosine analogs toward P-gp, the extended 3-substituted benzyl and 3,4-difluorophenyl moieties are required.

TABLE 3
Effect of adenosine (N)-methanocarba and riboside derivatives, including prototypical A$_3$ adenosine receptor agonists 22 and 23, on the ATPase activity of P-gp

Effect of various intact and truncated adenosine (N)-methanocarba and riboside derivatives, including prototypical A$_3$ adenosine receptor agonists **22** and **23**, on the ATPase activity of P-gp. ATPase activity was measured in total membranes prepared from High-Five insect cells expressing wild-type or mutant P-gp. Mean ± S.D. values represent the average of three independent experiments performed in duplicate. The values in the ATPase activity column indicate stimulation (upward arrows) of basal ATPase activity. ND, not determined; NE, no effect. Please see the legend to Table 1 for other details.

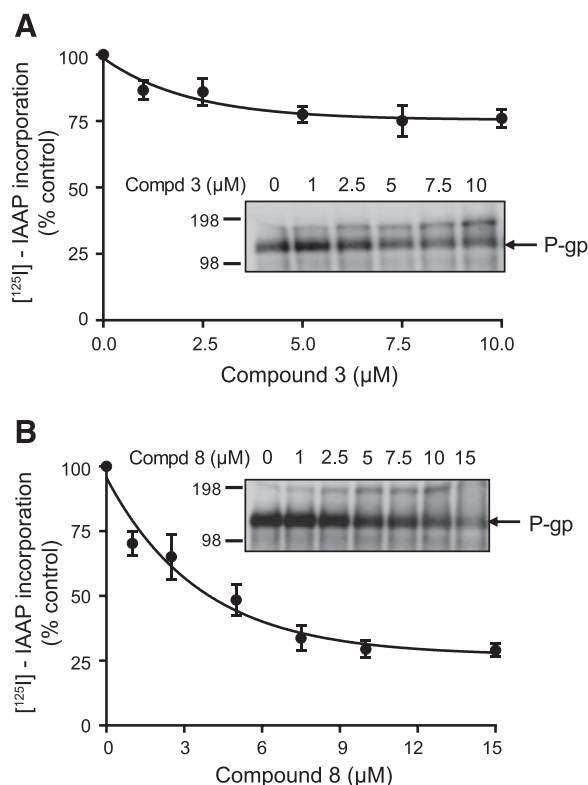| No.	Structure	ATPase Activity of P-gp % Stimulation or Inhibition	
		2.5 μM	10 μM
18		NE	ND
19		115.5 ± 4.9 ↑	NE
20		NE	ND
21		37.8 ± 5.0 ↑	ND
22		NE	NE
23		NE	79.9 ± 12.8 ↑

Fig. 4. Effect of compounds 3 and 8 on the photoaffinity labeling of P-gp by [^{125}I]iodoarylazidoprazosin. Total membranes of human P-gp–expressing High-Five insect cells (60 μg of protein per 100-μl volume) were incubated for 5 minutes, with increasing concentrations of compound 3 (A) 0–10 μM and 8 (B) 0–15 μM and later transferred to a 4°C water bath, followed by photo-crosslinking with ^{125}IAAP (3–4 nM) using 366 nm UV light for 10 minutes. The P-gp bands were separated using gel electrophoresis on 7% Tris-acetate gels. The gels were dried and exposed to X-ray films. Autoradiograms of IAAP-labeled P-gp bands using compounds 3 (A) and 8 (B) are shown. The curves were plotted using GraphPad Prism 7.0 with nonlinear one-phase exponential decay analysis. The values were obtained in three independent experiments carried out in duplicate. The value of IC$_{50}$ (compound concentration that produces 50% inhibition of IAAP incorporation into P-gp) is given as IC$_{50}$ = 3.65 ± 0.05 μM for compound 8 (B). IC$_{50}$ value was calculated using GraphPad Prism 7.0.

Current Food and Drug Administration guidelines for drug development recommend that investigational drugs be evaluated in vitro to determine whether they are potential substrates or inhibitors of P-gp. For this reason, we tested two adenosine analogs (22 and 23) currently in phase 2 and 3 clinical trials (David et al., 2012; Stemmer et al., 2013). Compound 22, riboside N^6-(3-iodobenzyl)-5′-N-methylcarboxamido adenosine, and its 2-chloro analog 23 were tested for their effect on ATPase activity. Compound 22 showed loss of affinity toward P-gp, and its 2-chloro derivative 23 at 10 μM stimulated ATPase activity in a concentration-dependent manner (see Supplemental Fig. 3). The structural basis for the distinction between these nucleosides in their interaction with P-gp is the presence of a 2-chlorine atom in compound 23, which is hydrogen in 22. These results could be due to the flexible nature of P-gp, which enables the protein to recognize various sizes and types of chemical structures (Patel et al., 2018); however, it should be noted that the affinity of both nucleosides at the target A$_3$ adenosine receptor is ~1 nM, and selectivity for the clinically relevant pathway is unchanged.

Effect of Adenosine Receptor Agonists on Photolabeling of P-gp with ^{125}I-Iodoarylazidoprazosin. To
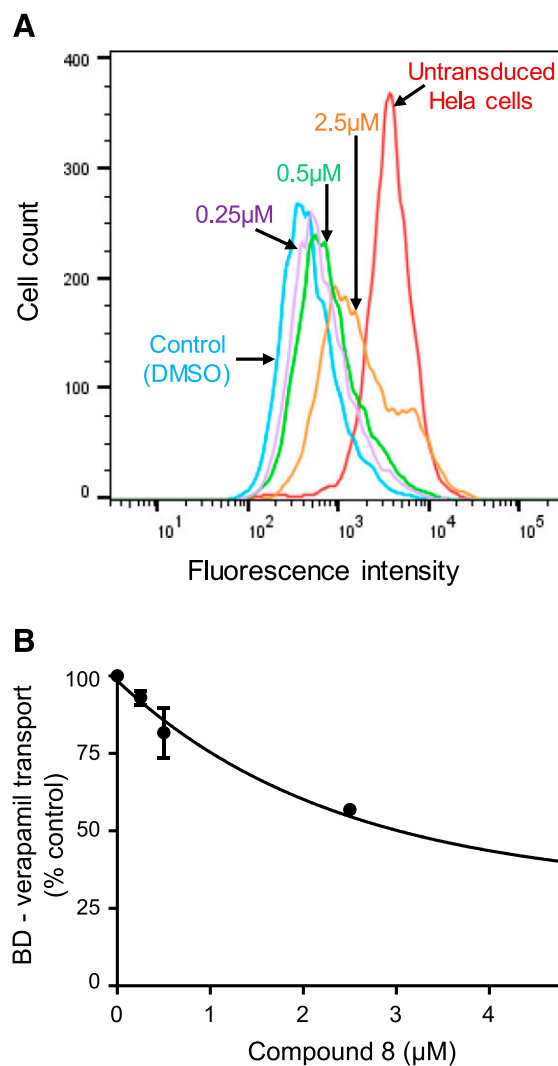

Fig. 5. Compound 8 inhibits substrate transport mediated by P-gp. Bac-Mam P-gp baculovirus-transduced HeLa cells were assayed for BD-verapamil (0.5 μM) transport, as described previously (Vahedi et al., 2017). (A) Representative histogram showing the effect of compound 8 at indicated concentrations on reversal of BD-verapamil transport by P-gp. (B) Concentration-dependent inhibition of BD-verapamil efflux by compound 8. In the plot (B), transport of BD-verapamil in the absence of compound 8 was taken as 100%, and the percentage of transport in the presence of compound 8 was calculated with respect to it. Data points are plotted as the mean ± S.D. (n = 3). The value of IC$_{50}$ (compound concentration that produces 50% inhibition of BD-verapamil transport in HeLa cells expressing P-gp) is given as IC$_{50}$ = 2.4 ± 0.6 μM.

determine whether compound 3 (strong stimulator) or 8 (partial inhibitor) interacts with P-gp at its drug-binding site, we determined the effect of these compounds on photolabeling of P-gp with IAAP, which is a transport substrate of this transporter (Maki et al., 2003). As shown in Fig. 4A, compound 3 partially inhibited (20%–25%) the photoaffinity labeling of P-gp with IAAP, even at a 10 μM concentration. Compound 8, on the other hand, inhibited covalent labeling of P-gp with IAAP in a concentration-dependent fashion with IC$_{50}$ value of 3.65 ± 0.05 μM (Fig. 4B).

Compound 8 Inhibits Substrate Transport Mediated by P-gp. The transport function was determined by an accumulation assay using a fluorescent substrate (BD-verapamil) at steady-state condition. The BD-verapamil is

normally transported by P-gp, so the effect of compound **8** (partial inhibitor) to reverse BD-verapamil transport was determined. At a 5 μM concentration, compound **8** was able to partially inhibit the transport of BD-verapamil by P-gp as shown in Fig. 5, with an IC$_{50}$ value of 2.4 $\pm$ 0.6 μM.

Interaction of Compound 3 with Residues in the Drug-Binding Pocket of P-gp. Examination of a recent cryoelectron microscopy structure of Taxol-bound human P-gp (Alam et al., 2019) (PDB: 6QEX) revealed 26 residues interacting with the ligand (within $\leq$4.0 Å). The results from the docking simulations with compound **3** in the structure of human P-gp revealed 11 residues that occur in at least 12 of the top 20 poses that are the same as for Taxol (see Supplemental Table 1). Figure 6A shows the best binding pose with lowest energy score for Compound **3**, and Supplemental Fig. 6A shows the superposition of the top 20 poses. From this, and additional docking simulations with Taxol, we chose an initial set of five residues to mutate to alanine and investigated their effect on ATPase activity (i.e., Y310, F336, F728, Y953, F983). In addition, F343 was mutated to cysteine and tyrosine to determine the effect of the thiol or hydroxyl groups on the interaction with A₃ adenosine receptor agonists. As seen in Table 4, for some of the single mutants (Y310A, F343Y, and F728A), compound **3** stimulated the basal ATPase activity, similar to its stimulation of wild-type P-gp; however, as suggested by the range of docked conformations (Supplemental Fig. 6A) and the flexible nature of the transmembrane region, compound **3** may bind in different configurations in the same protein pocket, indicating that it will be difficult to conclude with certainty that interaction with any single residue is critical. Consistent with these results, compound **3** also did not have any effect on the ATPase activity of a triple mutant with substitution of Y307, Q725, and F953 in the drug-binding pocket of P-gp to alanine (Y307A/Q725A/F953A; triple A mutant).

Interaction of Compound 8 with Residues in the Drug-Binding Pocket of P-gp. The same method used for the docking of compound **3** was also used for compound **8**. Supplemental Table 2 shows that 23 of 26 residues interact with both compound **8** and Taxol. Residues Y307, Y310, F336, F343, Q725, F728, and F983 interacted with compound **8** in more than 16 poses. For this reason, these residues were mutated to alanine. In addition, residue Y953 was added, based on the results obtained with compound **3**. As shown in Table 1, compound **8** partially inhibits the basal ATPase activity of wild-type P-gp (35% at 2.5 μM). As observed for compound **3**, residues selected for mutagenesis are likely to be involved in interaction with compound **8** (Table 5). As multiple residues in the drug-binding pocket appear to interact with this compound (based on the cluster of 20 poses shown in Supplemental Fig. 6B), when a single residue is mutated, other residues might compensate for it.

Interaction of Conjugated BODIPY-FL Compound (24) with P-gp. To assess the interaction of the fluorescent probe-conjugated compound (**24**), which was structurally derived from compound **8**, at the transmembrane domains of P-gp, its biochemical properties were characterized using an ATPase assay and in IAAP photoaffinity labeling of P-gp. The effect of BODIPY-FL-labeled compound **24** on the basal ATPase activity of P-gp was investigated in native membranes of High-Five insect cells expressing the protein. The BODIPY-FL-compound **24** showed weak inhibition (30%–35%) of basal ATPase activity of P-gp (Supplemental Fig. 4A). This result was similar to that of its parent compound (**8**). In the binding competition assay, shown
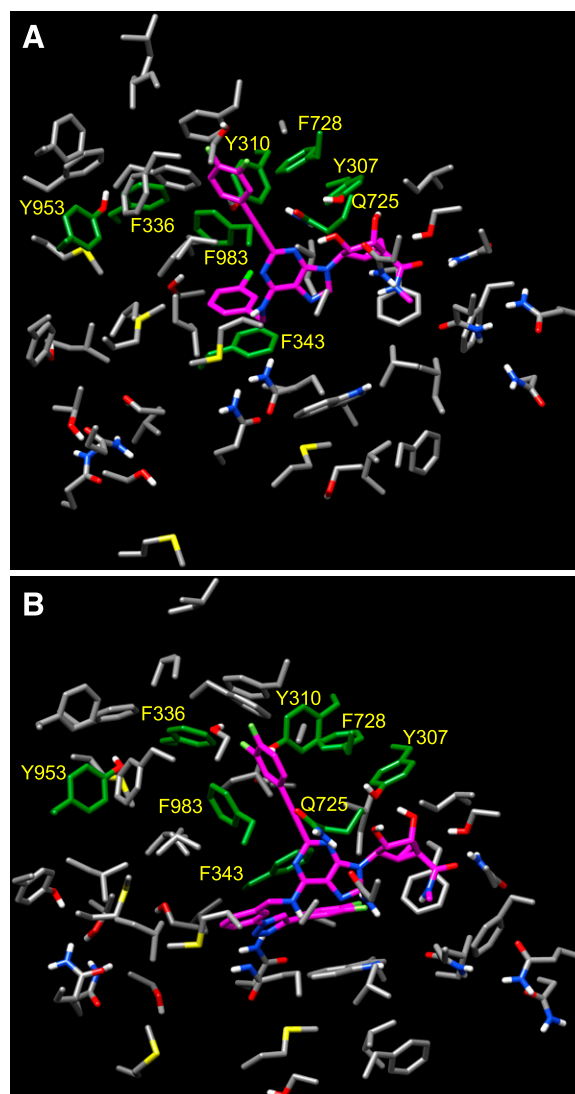

Fig. 6. Docking of compounds 3 (A) and 8 (B) in the drug-binding pocket of human P-gp. In the docking studies using the structure of Taxol-bound human P-gp (pdb.6QEX), we obtained the 20 best, lowest-energy, Vina poses for each compound. Whereas only the best pose for each is presented here for clarity, superpositions of all 20 are shown in Supplemental Fig. 6 to assess structural variation. The color code is as follows: nitrogen, blue; oxygen, red; hydrogen, white; sulfur, yellow; fluorine, chartreuse; and chlorine, light green. The carbons of the ligands are colored magenta, those of the mutated residues, dark green; and gray for the rest of the residues. The residues selected for substitution are labeled.

earlier in Fig. 4B, pretreatment of the native membranes with parent compound **8** in a concentration-dependent manner inhibited the photoaffinity labeling of P-gp with IAAP (IC$_{50}$ 3.65 $\pm$ 0.05 μM); however, we observed weak inhibition (20%–25%) of IAAP even at 15 μM for BODIPY-FL-compound **24** (Supplemental Fig. 4B). The reason for this change of affinity is likely the larger size of this conjugated fluorescent probe (**24**) compared with compound **8**, making it unable to bind at the high-affinity site of P-gp for steric reasons.

Discussion

P-gp exhibits polyspecificity and can transport a wide range of substrates. Recently, we reported that the interaction of

TABLE 4

Interaction of compound 3 with residues in the drug-binding pocket of P-gp

A summary of the interaction of compound **3** with residues in the drug-binding pocket of P-gp. Modulation of the basal ATPase activity of mutant P-gps by compound **3** was done at 2.5 and 5 μM. The percentage stimulation or inhibition by compound **3** is shown, and ATPase activities were determined as described in *Materials and Methods*. ATPase activity was measured in total membranes prepared from High-Five insect cells expressing mutant P-gp. Basal ATPase activity is considered as 0%. The values in the ATPase activity column indicate stimulation (upward arrows) or inhibition (downward arrows) of basal ATPase activity. The values represent the mean $\pm$ S.D. from three independent experiments (except for F343Y mutant, the average of two independent experiments is given).

P-gp Variant	ATPase Activity % Stimulation or Inhibition		Comment
	2.5 μM	5 μM	
Wild-type	88.3 $\pm$ 14.0 ↑	62.1 $\pm$ 7.9 ↑	Stimulation
F336A	NE	NE	No effect
F728A	39.1 $\pm$ 7.4 ↑	NE	Stimulation at 2.5 μM
F983A	NE	NE	No effect
Y953A	NE	39.4 $\pm$ 5.3 ↓	Inhibition at 5 μM
Y310A	40.1 $\pm$ 5.2 ↑	53.2 $\pm$ 14.8 ↑	Stimulation
Triple A	NE	NE	No effect
F343C	NE	NE	No effect
F343Y	54.2 ↑	NE	Stimulation at 2.5 μM

Triple A, Y307A/Q725A/Y953A; NE, no effect.

substrates with P-gp depends on their interactions with a pair of phenylalanine-tyrosine structural motifs in the substrate-binding pocket of the protein (Chufan et al., 2016). In that study, we reported that the phenylalanine residues F978 and F728 interact with tyrosine residues Y953 and Y310 in an edge-to-face conformation. This change in conformation orients the tyrosine residues in such a way that they establish hydrogen-bond contacts with known inhibitors, such as tariquidar, zosuquidar, and elacridar (Chufan et al., 2016). Most of these residues are located in pharmacologically distinct binding sites within the drug-binding pocket for compounds such as propafenones (interacting with Y953) (Dönmez Cakil et al., 2014) and rhodamine 123 (interacting with Y953 and F978) (Dönmez Cakil et al., 2014; Mittra et al., 2017).

In this regard, to evaluate the interaction of adenosine analogs with P-gp at the drug-binding pocket, as revealed in docking studies shown in Fig. 6, biochemical assays, including ATPase activity of P-gp and photolabeling of P-gp with IAAP, were performed. Figure 7 is a schematic representation of how adenosine analogs affect the ATPase activity of P-gp. Most adenosine receptor ligands neither stimulate nor inhibit the basal ATPase activity, suggesting the loss of their affinity toward P-gp; however, compounds **3** and **8** displayed pronounced effects on P-gp function. Compound **3** was observed to stimulate the basal ATPase activity of P-gp by up to 2-fold at concentrations ranging from 2.5 to 5.0 μM (Fig. 3A). This stimulation was possible owing to the presence of N^6-(3-chlorobenzyl) at the R^1 position of the adenine moiety, and 3,4-difluorophenyl at the R^2 position (Fig. 3C). Similar analogs with some chemical features in common with compound **3**, such as compounds **1**, **19**, **13**, and **15**, were also observed to stimulate the ATPase activity of P-gp. Second, compound **8** was observed to partially inhibit the basal ATPase activity of P-gp. This compound was designed to have structural features identical to known high-affinity inhibitors of P-gp, such as tariquidar, zosuquidar, and elacridar. We speculated that compound **8**, which has an extended 3-substituted benzyl at position R^1, and a 3,4-difluorophenyl at R^2, increases the hydrogen bonding or π-π interactions with residues in the drug-binding pocket of P-gp. Furthermore, we can see from Fig. 3B that compound **8** partially inhibited the basal ATPase activity of P-gp in a concentration-dependent manner. Similar

analogs, such as compounds **9**, **10**, and **11,** with some chemical features common with compound **8**, all weakly inhibited the ATPase activity of P-gp (Supplemental Fig. 1). We further evaluated the ability of compound **3** or **8** to inhibit the binding of another ligand IAAP, which is transported by P-gp (Maki et al., 2003). As shown in Fig. 4A, compound **3** partially inhibited (20%–25%) the photoaffinity labeling of P-gp with IAAP, even at a 10 μM concentration. Compound **8**, on the other hand, inhibited covalent labeling of P-gp with IAAP in a concentration-dependent fashion with an IC$_{50}$ of 3.65 $\pm$ 0.05 μM (Fig. 4B). This result clearly demonstrates that compound **8** can compete for photoaffinity labeling of P-gp with IAAP.

Additionally, compound **8** was evaluated for its ability to inhibit the transport function of human P-gp in HeLa cells. The transport function was determined by an accumulation assay using the fluorescent substrate BD-verapamil, which accumulates in the cells owing to inhibition of P-gp efflux by compound **8**. Figure 5A is a representative histogram showing that compound **8** partially inhibits the transport of BD-verapamil

TABLE 5

Alanine substitution of residues of drug-binding pocket interacting with compound 8 alters effect on ATPase activity of P-gp

Summary of the interaction of compound **8** with residues in the transmembrane region of P-gp. The effect of compound **8** on the basal ATPase activity of mutant P-gps was tested at 2.5 and 5 μM. As in Table 4, the percentage of stimulation or inhibition by compound **8** is shown and basal ATPase activity is considered 0%. ATPase activity was measured in total membranes prepared from High-Five insect cells expressing mutant P-gp. The values indicate stimulation (upward arrows) or inhibition (downward arrows) of basal ATPase activity (mean $\pm$ S.D. from three independent experiments, except for F343Y mutant, in which the average of two independent experiments is given).

P-gp variant	ATPase activity % Stimulation or Inhibition		Comment
	2.5 μM	5 μM	
Wild-type	35.5 $\pm$ 4.4 ↓	48.2 $\pm$ 12.3 ↓	Inhibition
F336A	NE	48.5 $\pm$ 5.9 ↑	Partial stimulation
F728A	NE	NE	No effect
F983A	NE	NE	No effect
Y953A	NE	47.3 $\pm$ 5.9 ↓	Inhibition at 5 μM
Y310A	39.5 $\pm$ 11.7 ↑	NE	No effect
Triple A	NE	NE	No effect
F343C	63.3 $\pm$ 1.1 ↓	62.6 $\pm$ 2.9 ↓	Inhibition
F343Y	58.0 ↓	56.7 ↓	Inhibition

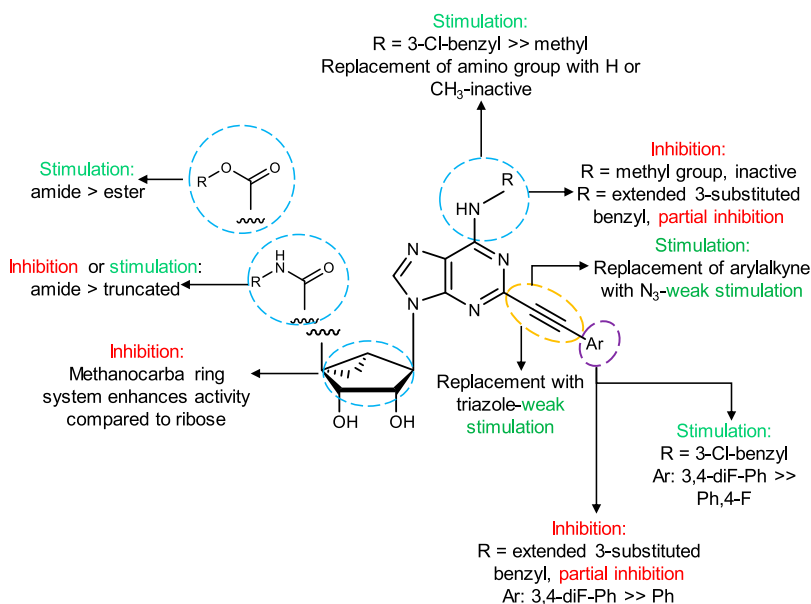Triple A, Y307A/Q725A/Y953A; NE, no effect.

Fig. 7. Schematic representation of the modulatory effect of tested A3 adenosine receptor agonist nucleosides on the ATPase activity of human P-gp. See the *Discussion* section for details.

with an IC$_{50}$ value of 2.4 $\pm$ 0.6 μM. The observed inhibitory effect could be due to the molecular framework of the adenosine analog. As shown in Fig. 3D, compound **8** was synthesized with an extended 3-substituted benzyl at position R^1 and with a 3, 4-difluorophenyl at R^2, which increases hydrogen bonding or π-π interactions with the protein and plays a critical role in the inhibition of P-gp transport function. Additionally, we decided to synthesize a fluorescent probe–conjugated compound (**24**) using click chemistry coupling (Fig. 2), which was structurally derived from compound **8**. This BODIPY-FL-labeled compound (**24**) was evaluated for its ability to interact with the drug-binding pocket of P-gp. Biochemical assays, such as ATPase activity and photolabeling of P-gp with IAAP, were performed (Supplemental Fig. 4). The BODIPY-FL-compound **24** weakly inhibited (30%–35%) the basal ATPase activity of P-gp (Supplemental Fig. 4A), which was similar to the activity of the parent compound (**8**); however, we observed weak inhibition (20%–25%) of IAAP incorporation into P-gp, even at 15 μM (Supplemental Fig. 4B). We then evaluated whether the BODIPY-FL-labeled compound (**24**) could be transported by P-gp; however, P-gp was unable to transport this fluorescent probe when used at concentrations ranging from 0.05 to 2.5 μM (Supplemental Fig. 5).

To identify residues located in the drug-binding pocket of P-gp interacting with selected adenosine analogs (compounds **3** and **8**), docking studies were performed using the recently solved structure of Taxol-bound human P-gp (Alam et al., 2019). Taxol-bound P-gp showed interaction of the ligand with 26 residues in the drug-binding pocket of the transporter. We compared the residues interacting with compounds **3**, **8**, and Taxol using data from the 6QEX structure ($\leq$4.0 Å); 18 of 26 residues showed interaction with both compound **3** and Taxol, whereas 23 of 26 residues are common with compound **8** and Taxol. The docking studies indicate that both compounds **3** and **8** bind in the same region of the drug-binding pocket as Taxol.

Although the mutagenesis of some of the residues supports the conclusion that both compounds **3** and **8** bind in the drug-binding pocket similar to the transport substrate Taxol, it is

difficult to identify individual residues which are critical for binding of these compounds with certainty owing to the flexible nature of the transmembrane region (Vahedi et al., 2017) and because in silico docking simulations showed a cluster of multiple possible conformations of these compounds in the same region (Supplemental Fig. 6, A and B). When a single residue is mutated, other residues in the drug-binding pocket might compensate for it.

In summary, 23 adenosine receptor ligands were synthesized to evaluate their interaction within the TMDs of P-gp, and their effect on basal ATPase activity was determined. Most adenosine receptor ligands showed neither stimulation nor inhibition of the basal ATPase activity, suggesting the loss of interaction with P-gp; however, compound **3** stimulated the ATPase activity of P-gp up to 2-fold, largely owing to the presence of the chlorobenzene ring. On the other hand, compound **8** partially inhibited the basal ATPase activity of P-gp owing to the presence of the fluoro group and an extended 3-substituted benzyl. Thus, this study indicates that A$_3$ adenosine receptor agonists can exhibit varied modulatory effects on P-gp activity, depending on structural functionalization. Our efforts in the next phase of study will focus on optimization of compound **8** to obtain not only a highly potent P-gp inhibitor but also to develop analogs to enhance the A$_3$ adenosine receptor selectivity.

References

Alam A, Kowal J, Broude E, Roninson I, and Locher KP (2019) Structural insight into substrate and inhibitor discrimination by human P-glycoprotein. *Science* **363**: 753–756.

Ambudkar SV (1998) Drug-stimulatable ATPase activity in crude membranes of human MDR1-transfected mammalian cells. *Methods Enzymol* 292:504–514.

Ambudkar SV, Dey S, Hrycyna CA, Ramachandra M, Pastan I, and Gottesman MM (1999) Biochemical, cellular, and pharmacological aspects of the multidrug transporter. *Annu Rev Pharmacol Toxicol* 39:361–398.

Chufan EE, Kapoor K, and Ambudkar SV (2016) Drug-protein hydrogen bonds govern the inhibition of the ATP hydrolysis of the multidrug transporter P-glycoprotein. *Biochem Pharmacol* 101:40–53.

Chufan EE, Kapoor K, Sim H-M, Singh S, Talele TT, Durell SR, and Ambudkar SV (2013) Multiple transport-active binding sites are available for a single substrate on human P-glycoprotein (ABCB1). *PLoS One* 8:e82463.

David M, Akerman L, Ziv M, Kadurina M, Gospodinov D, Pavlotsky F, Yankova R, Kouzeva V, Ramon M, Silverman MH, et al. (2012) Treatment of plaque-type psoriasis with oral CF101: data from an exploratory randomized phase 2 clinical trial. *J Eur Acad Dermatol Venereol* 26:361–367.

Dönmez Cakil Y, Khunweeraphong N, Parveen Z, Schmid D, Artaker M, Ecker GF, Sitte HH, Pusch O, Stockner T, and Chiba P (2014) Pore-exposed tyrosine residues of P-glycoprotein are important hydrogen-bonding partners for drugs. *Mol Pharmacol* 85:420–428.

Gottesman MM and Pastan I (1993) Biochemistry of multidrug resistance mediated by the multidrug transporter. *Annu Rev Biochem* 62:385–427.

Kapoor K, Bhatnagar J, Chufan EE, and Ambudkar SV (2013) Mutations in intracellular loops 1 and 3 lead to misfolding of human P-glycoprotein (ABCB1) that can be rescued by cyclosporine A, which reduces its association with chaperone Hsp70. *J Biol Chem* 288:32622–32636.

Kerr KM, Sauna ZE, and Ambudkar SV (2001) Correlation between steady-state ATP hydrolysis and vanadate-induced ADP trapping in Human P-glycoprotein. Evidence for ADP release as the rate-limiting step in the catalytic cycle and its modulation by substrates. *J Biol Chem* 276:8657–8664.

Leslie EM, Deeley RG, and Cole SP (2005) Multidrug resistance proteins: role of P-glycoprotein, MRP1, MRP2, and BCRP (ABCG2) in tissue defense. *Toxicol Appl Pharmacol* 204:216–237.

Maki N, Hafkemeyer P, and Dey S (2003) Allosteric modulation of human P-glycoprotein: inhibition of transport by preventing substrate translocation and dissociation. *J Biol Chem* 278:18132–18139.

Mittra R, Pavy M, Subramanian N, George AM, O'Mara ML, Kerr ID, and Callaghan R (2017) Location of contact residues in pharmacologically distinct drug binding sites on P-glycoprotein. *Biochem Pharmacol* 123:19–28.

Patel BA, Abel B, Barbuti AM, Velagapudi UK, Chen Z-S, Ambudkar SV, and Talele TT (2018) Comprehensive synthesis of amino acid-derived thiazole peptidomimetic analogues to understand the enigmatic drug/substrate-binding site of P-glycoprotein. *J Med Chem* 61:834–864.

Ramachandra M, Ambudkar SV, Chen D, Hrycyna CA, Dey S, Gottesman MM, and Pastan I (1998) Human P-glycoprotein exhibits reduced affinity for substrates during a catalytic transition state. *Biochemistry* 37:5010–5019.

Sauna ZE and Ambudkar SV (2000) Evidence for a requirement for ATP hydrolysis at two distinct steps during a single turnover of the catalytic cycle of human P-glycoprotein. *Proc Natl Acad Sci USA* 97:2515–2520.

Sauna ZE, Nandigama K, and Ambudkar SV (2006) Exploiting reaction intermediates of the ATPase reaction to elucidate the mechanism of transport by P-glycoprotein (ABCB1). *J Biol Chem* 281:26501–26511.

Shukla S, Schwartz C, Kapoor K, Kouanda A, and Ambudkar SV (2012) Use of baculovirus BacMam vectors for expression of ABC drug transporters in mammalian cells. *Drug Metab Dispos* 40:304–312.

Stemmer SM, Benjaminov O, Medalia G, Ciuraru N, Silverman MH, Yehuda SB, Fishman S, Harpaz Z, Farbstein M, Cohen S, et al. (2013) CF102 for the treatment of hepatocellular carcinoma: a phase I/II, open-label, dose-escalation study. *Oncologist* 18:25–26.

Tosh DK, Ciancetta A, Warnick E, O'Connor R, Chen Z, Gizewski E, Crane S, Gao Z-G, Auchampach JA, Salvemini D, et al. (2016) Purine (N)-methanocarba nucleoside derivatives lacking an exocyclic amine as selective A3 adenosine receptor agonists. *J Med Chem* 59:3249–3263.

Tosh DK, Crane S, Chen Z, Paoletta S, Gao Z-G, Gizewski E, Auchampach JA, Salvemini D, and Jacobson KA (2015a) Rigidified A3 adenosine receptor agonists: 1-deazaadenine modification maintains high in vivo efficacy. *ACS Med Chem Lett* 6:804–808.

Tosh DK, Deflorian F, Phan K, Gao Z-G, Wan TC, Gizewski E, Auchampach JA, and Jacobson KA (2012a) Structure-guided design of A(3) adenosine receptor-selective nucleosides: combination of 2-arylethynyl and bicyclo[3.1.0]hexane substitutions. *J Med Chem* 55:4847–4860.

Tosh DK, Finley A, Paoletta S, Moss SM, Gao Z-G, Gizewski ET, Auchampach JA, Salvemini D, and Jacobson KA (2014a) In vivo phenotypic screening for treating chronic neuropathic pain: modification of C2-arylethynyl group of conformationally constrained A3 adenosine receptor agonists. *J Med Chem* 57:9901–9914.

Tosh DK, Janowsky A, Eshleman AJ, Warnick E, Gao Z-G, Chen Z, Gizewski E, Auchampach JA, Salvemini D, and Jacobson KA (2017) Scaffold repurposing of nucleosides (adenosine receptor agonists): enhanced activity at the human dopamine and norepinephrine sodium symporters. *J Med Chem* 60:3109–3123.

Tosh DK, Padia J, Salvemini D, and Jacobson KA (2015b) Efficient, large-scale synthesis and preclinical studies of MRS5698, a highly selective A3 adenosine receptor agonist that protects against chronic neuropathic pain. *Purinergic Signal* 11:371–387.

Tosh DK, Paoletta S, Chen Z, Crane S, Lloyd J, Gao Z-G, Gizewski ET, Auchampach JA, Salvemini D, and Jacobson KA (2015c) Structure-based design, synthesis by click chemistry and in vivo activity of highly selective A3 adenosine receptor agonists. *MedChemComm* 6:555–563.

Tosh DK, Paoletta S, Chen Z, Moss SM, Gao Z-G, Salvemini D, and Jacobson KA (2014b) Extended N(6) substitution of rigid C2-arylethynyl nucleosides for exploring the role of extracellular loops in ligand recognition at the A3 adenosine receptor. *Bioorg Med Chem Lett* 24:3302–3306.

Tosh DK, Paoletta S, Phan K, Gao Z-G, and Jacobson KA (2012b) Truncated nucleosides as A(3) adenosine receptor ligands: combined 2-arylethynyl and bicyclohexane substitutions. *ACS Med Chem Lett* 3:596–601.

Trott O and Olson AJ (2010) AutoDock Vina: improving the speed and accuracy of docking with a new scoring function, efficient optimization, and multithreading. *J Comput Chem* 31:455–461.

Vahedi S, Chufan EE, and Ambudkar SV (2017) Global alteration of the drug-binding pocket of human P-glycoprotein (ABCB1) by substitution of fifteen conserved residues reveals a negative correlation between substrate size and transport efficiency. *Biochem Pharmacol* 143:53–64.

Address correspondence to: Kenneth A. Jacobson, Molecular Recognition Section, Laboratory of Bioorganic Chemistry, National Institute of Diabetes and Digestive and Kidney Diseases Building 8A, Room B1A19, 8 Center Drive, Bethesda, MD 20814. E-mail: kennethj@niddk.nih.gov; or Suresh V. Ambudkar, Laboratory of Cell Biology, Center for Cancer Research, National Cancer Institute, NIH, Building 37, Room 2120, 37 Convent Dr., Bethesda, MD 20892. E-mail: ambudkar@mail.nih.gov